Inorg. Chem. **2008**, *47*, 10141−10149

The First Dinitrile Frameworks of the Rare Earth Elements: $^3_\infty$[LnCl$_3$(1,4-Ph(CN)$_2$)] and $^3_\infty$[Ln$_2$Cl$_6$(1,4-Ph(CN)$_2$)], Ln = Sm, Gd, Tb, Y; Access to Novel Metal-Organic Frameworks by Solvent Free Synthesis in Molten 1,4-Benzodinitrile

Christoph J. Höller and Klaus Müller-Buschbaum*

Department Chemie and Biochemie, Ludwig-Maximilians-Universität München, Butenandtstrasse 5-13, D-81377 München, Germany

Received April 10, 2008

The three-dimensional frameworks $^3_\infty$[LnCl$_3$(1,4-Ph(CN)$_2$)] of the lanthanides Ln = Sm (**1**), Gd (**2**), Tb (**3**), and $^3_\infty$[Ln$_2$Cl$_6$(1,4-Ph(CN)$_2$)] for the group 3 metal Y (**4**) were obtained as single crystalline materials by the reaction of the anhydrous chlorides of the referring rare earth elements with a melt of 1,4-benzodinitrile. No additional solvents were used for the reactions. The dinitrile ligand is strongly coordinating and substitutes parts of the chlorine coordination. The Ln halide structures are reduced to two-dimensional networks, whereas coordination of both nitrile functions to the metal ions renders bridging in the third direction accessible. This enables formation of new metal organic framework (MOF) structure types with the large 1,4-benzodinitrile spacers interlinking $^2_\infty$[LnCl$_3$] planes. In comparison to 1,4-Ph(CN)$_2$ the mono functional benzonitrile ligand does not constitute framework structures, which is underlined by comparison with a reaction of yttrium chloride with PhCN resulting in the molecular complex [Y$_2$Cl$_6$(PhCN)$_6$] (**5**) with end-on coordination PhCN ligands. The coordination spheres of the rare earth ions consist of double capped ($^3_\infty$[LnCl$_3$(1,4-Ph(CN)$_2$)] (**1**−**3**)) as well as single capped trigonal prisms ($^3_\infty$[Ln$_2$Cl$_6$(1,4-Ph(CN)$_2$)] (**4**)) of chloride ions and N≡C groups while **5** displays edge sharing pentagonal bipyramids as coordination polyhedra. Sm (**1**), Gd (**2**), and Tb (**3**) exhibit isotypic framework structures with intercrossing dinitrile ligands. The group 3 metal Y (**4**) gives a framework with a coplanar arrangement of ligands and a lower ligand content. The largest cavities within the MOF structures of **1**−**4** have diameters of 3.9−8.0 Å. All compounds were identified by single crystal X-ray analysis. Mid IR, Far IR, and Raman spectroscopy, microanalyses and simultaneous Differential Thermal Analysis-Thermogravimetry (DTA/TG) were also carried out to characterize the products. Crystal data for $^3_\infty$[LnCl$_3$(1,4-Ph(CN)$_2$)] (**1**−**3**): *Pnma*, T = 170(2) K; Sm (**1**): a = 7.172(1) Å, b = 22.209(3) Å, c = 6.375(1) Å, V = 1015.4(3) Å^3, R$_1$ for $F_o > 4\sigma(F_o)$ = 0.032, wR$_2$ = 0.079. Gd (**2**): a = 7.116(1) Å, b = 22.147(4) Å, c = 6.345(1) Å, V = 1000.0(3) Å^3, R$_1$ for $F_o > 4\sigma(F_o)$ = 0.033, wR$_2$ = 0.085. Tb (**3**): a = 7.090(2) Å, b = 22.140(4) Å, c = 6.325(2) Å, V = 992.8(3) Å^3, R$_1$ for $F_o > 4\sigma(F_o)$ = 0.025, wR$_2$ = 0.061. Crystal data for $^3_\infty$[Y$_2$Cl$_6$(1,4-Ph(CN)$_2$)] (**4**): $P\bar{1}$, T = 170(2) K; a = 6.653(2) Å, b = 6.799(2) Å, c = 9.484(2) Å, V = 397.9(2) Å^3, R$_1$ for $F_o > 4\sigma(F_o)$ = 0.027, wR$_2$ = 0.069. Crystal data for [Y$_2$Cl$_6$(PhCN)$_6$] (**5**): $P2_1/c$, T = 170(2) K; a = 9.767 (2) Å, b = 12.304(3) Å, c = 19.110(4) Å, V = 2294.8(8) Å^3, R$_1$ for $F_o > 4\sigma(F_o)$ = 0.041, wR$_2$ = 0.092.

Introduction

The chemistry of coordination polymers and network structures is rapidly developing, especially the field of the metal organic frameworks (MOFs).[1−6] The interest in MOFs mainly derives from applicational aspects such as their use as porous materials for the storage of small molecules like

* To whom correspondence should be addressed. E-mail: kmbch@cup.uni-muenchen.de. Fax: 0049 (0)89 2180 77851.

(1) Hagrman, P. J.; Hagrman, D.; Zubieta, J. *Angew. Chem., Int. Ed.* **1999**, *38*, 2638–2684; *Angew. Chem.* **1999**, *111*, 2799−2848.

(2) Yaghi, O. M.; Li, H.; Davis, C.; Richardson, T.; Groy, T. L. *Acc. Chem. Res.* **1998**, *31*, 474–484.

(3) Blake, A. J.; Champness, N. R.; Hubberstey, P.; Li, W. S.; Withersby, M. A.; Schröder, M. *Coord. Chem. Rev.* **1999**, *183*, 117–138.

10.1021/ic800635u CCC: $40.75
Published on Web 10/08/2008

hydrogen, methane, or propane.[7−11] Besides other metals the work on rare earth elements has been tremendously increasing. Because of the high oxophilicity of the lanthanides most of them consist of oxygen coordinated frameworks and constitute of carboxylates and alcoholates.[12−22] Non-oxygen containing frameworks exhibit benefits like higher thermal endurance,[23−26] as they do not decarboxylate upon heating, which is desirable for withstanding sorption energies, but they are less easily accessible and so far limited to only a few rare earth amides of aromatic N heterocycles like imidazolate and triazolates.[23−26] To avoid any kind of oxygen containing ligand a solvent free synthesis strategy in the melt of the referring amine has been developed for the formation of amide coordination polymers as it prevents all kinds of unwanted co-coordination.[27−31] The basis of these reactions is a redox process reducing the amine and oxidizing a lanthanide metal; thus, redox inactive ligands have not yet been accessible to this kind of synthesis. To introduce functional groups like nitriles to high temperature melt syntheses suitable precursors are necessary. Reactions of water free rare earth halides with melts of benzodinitriles prove suitable to obtain framework structures and also lead to the first rare earth dinitrile MOFs. Even of transition metals, only few examples are known: some copper di- and tetranitrile networks as well as silver and rhodium polymers including various other ligands.[32−35] Here we present dinitrile MOFs of 1,4-Ph$(CN)_2$ together with trichlorides of samarium, gadolinium, terbium, and yttrium.

Experimental Section

General Data. All manipulations were carried out under inert atmospheric conditions using glovebox, Schlenk, Duran glass ampule as well as vacuum line techniques. Heating furnaces with Al_2O_3 tubes together with Eurotherm 2416 control elements were used for the ampule experiments. The reaction conditions giving **1**−**4** and **5** were adjusted to the aggregate states of the reagents: reactions for **1**−**4** consist of solid reagents only and were performed in the melt of the ligand, whereas the procedure for **5** contains liquid benzonitrile. The IR spectra were recorded using a Bruker FTIR-IS66V-S spectrometer, the Raman spectra using a Bruker FRA 106-S spectrometer. For Mid IR (MIR) investigations KBr pellets, for Far IR (FIR) PE pellets were used under vacuum. For thermal analysis and powder diffraction the products were purified by evaporating excess 1,4-$(Ph(CN)_2)$ at 200 °C. For microanalysis single crystals of **1**−**5** were used. The thermal decomposition of $^3_\infty$[$LnCl_3$(1,4-$Ph(CN)_2$)] was studied using simultaneous Differential Thermal Analysis-Thermogravimetry (DTA/TG) (Netzsch STA-409) on the samarium containing MOF **1** as an exemplary. A 32.7 mg quantity of **1** was heated from 20 to 700 °C in a constant Ar-flow of 60 mL/min with a heating rate of 15 °C/min.

The trichlorides $LnCl_3$, Ln = Sm, Gd, Tb, Y were prepared according to the ammonium halide route[36] using the oxides Ln_2O_3 (ChemPur, 99.9%), HCl solution (10 mol/L), and ammonium chloride (Fluka, 99.5%) and purified by decomposition of the trivalent ammonium chlorides and subsequent sublimation. PhCN (ACROS, 99%) was dried over CaH_2 and mole sieve. 1,4-$Ph(CN)_2$ (ACROS, 98%) was used as purchased. All products are air and moisture sensitive.

$^3_\infty$[$SmCl_3$(1,4-$Ph(CN)_2$)] (1). $SmCl_3$ (0.5 mmol = 128 mg) and 1,4-benzodinitrile (1,4-$Ph(CN)_2$, 1.5 mmol = 192 mg) were sealed in an evacuated Duran glass ampule and heated to 190 °C in 9.5 h and to 235 °C in another 45 h. This temperature was held for 48 h. The reaction mixture was then cooled to 190 °C over 225 h, to 170 °C in 20 h, and to room temperature within 29 h. The reaction resulted in highly reflecting transparent colorless crystals of the product next to the excess ligand and some SmOCl, which derives from the synthesis of $SmCl_3$. Yield: 164 mg = 85%. Anal. Calcd for $C_8Cl_3H_4N_2Sm$ (M_r = 384.85 g mol^{-1}): C, 24.96; N, 7.27; H, 1.05. Found: C, 25.09; N, 7.23; H, 0.96. MIR (KBr): (3039 w, 2260 m, 2233 m, 1633 m, 1498 m, 1401 vs, 1278 m, 1199 w, 1105 w, 1014 w, 849 s, 651 w, 542 s) cm^{-1}. FIR (PE): (542 m, 474 m, 275 m, 234 w, 207 w, 167 w, 154 w, 130 w) cm^{-1}. Raman:

(4) Batten, S. R.; Robson, R. *Angew. Chem., Int. Ed.* **1998**, *37*, 1460–1494; *Angew. Chem.* **1998**, *110*, 1558−1595.
(5) Eddaoudi, M.; Kim, J.; Wachter, J. B.; Chae, H. K.; O'Keeffe, M.; Yaghi, O. M. *J. Am. Chem. Soc.* **2001**, *123*, 4368–4369.
(6) Zheng, X.; Sun, C.; Lu, S.; Liao, F.; Goa, S.; Jin, L. *Eur. J. Inorg. Chem.* **2004**, 3262–3268.
(7) Le, H.; Eddaoudi, M.; O'Keefe, M.; Yaghi, O. M. *Nature* **1999**, *402*, 276–279.
(8) Ferey, G. *Chem. Mater.* **2001**, *13*, 3084–3098.
(9) Althues, H.; Kaskel, S. *Langmuir* **2002**, *18*, 7428–7435.
(10) Biradha, K.; Fujita, M. *Angew. Chem., Int. Ed.* **2002**, *41*, 3392–3395; *Angew. Chem.* **2002**, *114*, 3542−3545.
(11) Evans, O. R.; Xiong, R.; Wang, Z.; Wong, G. K.; Lin, W. *Angew. Chem., Int. Ed.* **1999**, *38*, 536–538; *Angew. Chem.* **1999**, *111*, 557−559.
(12) Wu, L. P.; Munakata, M.; Kuroda-Sowa, T.; Maekawa, M.; Suenaga, Y. *Inorg. Chim. Acta* **1996**, *249*, 183–189.
(13) Reineke, T. M.; Eddaoudi, M.; Fehr, M.; Kelley, D.; Yaghi, O. M. *J. Am. Chem. Soc.* **1999**, *121*, 1651–1657.
(14) Long, D.-L.; Blake, A. J.; Champness, N. R.; Wilson, C.; Schröder, M. *J. Am. Chem. Soc.* **2001**, *123*, 3401–3402.
(15) Long, D.-L.; Blake, A. J.; Champness, N. R.; Wilson, C.; Schröder, M. *Angew. Chem., Int. Ed.* **2001**, *40*, 2444–2447; *Angew. Chem.* **2001**, *113*, 2510−2513.
(16) Devic, T.; David, O.; Valls, M.; Marrot, J.; Couty, F.; Ferey, G. *J. Am. Chem. Soc.* **2007**, *129*, 12614–12615.
(17) Cao, R.; Sun, D. F.; Liang, Y. C.; Hong, M. C.; Tatsumi, K.; Shi, Q. *Inorg. Chem.* **2002**, *41*, 2087–2094.
(18) Kim, Y.; Jung, D.-Y. *J. Chem. Soc., Chem. Commun.* **2002**, 908–909.
(19) Zheng, X.; Sun, C.; Lu, S.; Liao, F.; Gao, S.; Jin, L. *Eur. J. Inorg. Chem.* **2004**, 3262–3268.
(20) Long, D.-L.; Blake, A. J.; Champness, N. R.; Wilson, C.; Schröder, M. *Chem. Soc., Chem. Commun.* **2000**, 1369–1370.
(21) Liu, J.; Meyer, E. A.; Cowan, J. A.; Shore, S. G. *Chem. Soc., Chem. Commun.* **1998**, 2043–2044.
(22) Wan, Y. H.; Zhang, L. P.; Jin, L. P.; Gao, S.; Lu, S. Z. *Inorg. Chem.* **2003**, *42*, 4985–4994.
(23) Müller-Buschbaum, K.; Mokaddem, Y. *J. Chem. Soc., Chem. Commun.* **2006**, 2060–2062.
(24) Müller-Buschbaum, K. *Z. Naturforsch.* **2006**, *61b*, 792–797.
(25) Müller-Buschbaum, K.; Gomez-Torres, S.; Larsen, P.; Wickleder, C. *Chem. Mater.* **2007**, *19*, 855–859.
(26) Müller-Buschbaum, K.; Mokaddem, Y. *Angew. Chem., Int. Ed.* **2007**, *46*, 4385–4387; *Angew. Chem.* **2007**, *119*, 4463−4466.
(27) Müller-Buschbaum, K. *Z. Anorg. Allg. Chem.* **2005**, *631*, 811–828.
(28) Müller-Buschbaum, K.; Quitmann, C. C. *Z. Anorg. Allg. Chem.* **2003**, *629*, 1610–1616.
(29) Müller-Buschbaum, K.; Quitmann, C. C. *Eur. J. Inorg. Chem.* **2004**, 4330–4337.
(30) Quitmann, C. C.; Müller-Buschbaum, K. *Z. Anorg. Allg. Chem.* **2005**, *631*, 1191–1198.
(31) Müller-Buschbaum, K.; Mokaddem, Y. *Eur. J. Inorg. Chem.* **2006**, 2000–2010.
(32) Carlucci, L.; Ciani, G. v.; Gudenberg, D. W.; Proserpio, D. M. *New J. Chem.* **1999**, *23*, 397–401.
(33) Niu, T.; Lu, J.; Grisci, G.; Jacobson, A. *Polyhedron* **1998**, *17*, 4079–4089.
(34) Munakata, M.; Ning, G. L.; Kurado-Sowa, T.; Maekawa, M.; Suenaga, Y.; Horino, T. *Inorg. Chem.* **1998**, *37*, 5651–5656.
(35) Venkatamaran, D.; Gardner, G. B.; Covey, A. C.; Lee, S.; Moore, J. S. *Acta Crystallogr.* **1996**, *C52*, 2416–2419.
(36) Meyer, G. *Inorg. Synth.* **1989**, *25*, 146–150.

(3084 m, 2277 vs, 2248 s, 1608 m, 1163 m, 810 w, 718 w, 547 m, 511 m, 412 w, 243 m, 225 m, 148 w) cm^{-1}.

$^3_\infty$[GdCl$_3$(1,4-Ph(CN)$_2$)] (2). $GdCl_3$ (0.5 mmol = 132 mg) and 1,4-benzodinitrile (1,4-$Ph(CN)_2$, 1.5 mmol = 192 mg) were sealed in an evacuated Duran glass ampule and treated as described for **1**. Except for an amount of unidentified secondary product and the excess ligand the reaction resulted in highly reflecting transparent colorless crystals of **2**. Yield: 161 mg = 82%. Anal. Calcd for $C_8Cl_3H_4N_2Gd$ (M_r = 391.74 g mol^{-1}): C, 24.52; N, 7.15; H, 1.03. Found: C, 24.39; N, 7.13; H, 1.87. MIR (KBr): (3173 m, 2263 m, 2233 s, 1631 m, 1548 w, 1498 w, 1400 s, 1278 m, 1201 w, 1105 w, 1017 m, 845 s, 813 wsh, 565 s) cm^{-1}. FIR (PE): (542 w, 478 w, 273 w, 229 w, 206 w, 186 w, 160 w, 142 w, 119 w,) cm^{-1}. Raman: 3069 w, 2261 vs, 1601 s, 1190 w, 1172 s, 822 w, 802 w, 723 w, 557 m, 519 m, 401 m, 254 w, 231 w, 218 w, 151 w, 131 w) cm^{-1}.

$^3_\infty$[TbCl$_3$(1,4-Ph(CN)$_2$)] (3). $TbCl_3$ (0.5 mmol = 133 mg) and 1,4-benzodinitrile (1,4-$Ph(CN)_2$, 1.5 mmol = 192 mg) were sealed in an evacuated Duran glass ampule and treated as described for **1** and **2**. The reaction formed a bulk of highly reflecting transparent light gray crystals of the product, excess ligand, and a slight amount of an unidentified secondary product observed by powder diffraction, which is different from **4**. Yield: 169 mg = 86%. Anal. Calcd for $C_8Cl_3H_4N_2Tb$ (M_r = 393.42 g mol^{-1}): C, 24.42; N, 7.12; H, 1.02. Found: C, 24.62; N, 7.06; H, 1.08. MIR (KBr): (3082 w, 2258 m, 2233 m, 1634 s, 1497 m, 1400 s, 1279 m, 1199 w, 1015 m, 986 w, 845 s, 779 w, 706 m, 563 s, 530 w,) cm^{-1}. FIR (PE): (566 m, 426 w, 279 w, 254 w, 232 w, 207 m, 160 w, 133 w, 112 w) cm^{-1}. Raman: (3068 w, 2260 vs, 1601 m, 1172 m, 557 w, 519 w, 401 w) cm^{-1}.

$^3_\infty$[Y$_2$Cl$_6$(1,4-Ph(CN)$_2$)] (4). YCl_3 (0.5 mmol = 98 mg) and 1,4-benzodinitrile (1,4-$Ph(CN)_2$, 1.5 mmol = 192 mg) were sealed in an evacuated Duran glass ampule and also treated as described for **1**−**3**. Highly reflecting transparent colorless crystals of **4** resulted in good yield from the reaction next to the excess ligand and an unidentified secondary phase, that is, different from **1**−**3**. The reaction was complete and resulted in the following. Yield: 223 mg = 86%. Anal. Calcd for $C_8Cl_6H_4N_2Y_2$ (M_r = 518.66 g mol^{-1}): C, 18.52; N, 5.40; H, 0.78. Found: C, 18.35; N, 5.37; H, 0.79. MIR (KBr): (3091 s, 2261 s, 1630 ssh, 1619 s, 1525 m, 1496 m, 1402 s, 1284 s, 1225 w, 1202 w, 1017 m, 849 s, 831 ssh, 665 m) cm^{-1}. FIR (PE): (566 vs, 550 m, 540 msh, 275 ssh, 224 s, 191 msh, 170 s, 125 w) cm^{-1}. Raman: (3078 w, 2277 vs, 2266 s, 1604 m, 1178 m, 817 w) cm^{-1}.

[Y$_2$Cl$_6$(PhCN)$_6$] (5). YCl_3 (0.72 mmol = 139 mg) and benzonitrile (PhCN), 4 mmol = 206 mg) were placed in a Duran glass ampule, frozen with liquid nitrogen, degassed, and sealed after evacuation. Highly reflecting transparent colorless crystals of the product formed without any heating at room temperature over 72 h. No products other than **5** and excess PhCN and YCl_3 were observed. Yield: 323 mg = 64%. Anal. Calcd for $C_{42}Cl_6H_{30}N_6Y_2$ (M_r = 1009.24 g mol^{-1}): C, 49.98; N, 8.33; H, 2.99. Found: C, 50.21; N, 8.29; H, 2.82. MIR (KBr): (3358 m, 3109 w, 3035 w, 2267 vs, 1595 m, 1487 m, 1446 s, 1293 w, 1201 w, 1176 m, 1164 w, 1094 w, 1068 w, 1028 w, 999 w, 761 vs, 683 s, 552 s, 492 m) cm^{-1}. FIR (PE): (552 m, 492 w, 389 w, 218 m, 150 w) cm^{-1}. Raman: 3070 m, 2264 vs, 1595 s, 1201 w, 1180 w, 1000 m, 762 w, 556 w, 491 w, 392 w, 249 w, 214 w, 144 w.

X-ray Crystallographic Studies. The best out of three single crystals of each of the compounds $^3_\infty$[LnCl$_3$(1,4-Ph(CN)$_2$)], Ln = Sm (**1**), Gd (**2**), $^3_\infty$[Y$_2$Cl$_6$(1,4-Ph(CN)$_2$)] (**4**), and the best out of seven crystals of $^3_\infty$[TbCl$_3$(1,4-Ph(CN)$_2$)] (**3**) and [Y$_2$Cl$_6$(PhCN)$_6$] (**5**) were selected for single crystal X-ray investigations under glovebox conditions and sealed in glass capillaries. All data collections were carried out on a STOE IPDS-II diffractometer at 170 K (Mo Kα radiation λ = 0.7107 Å). For all five compounds the structures were determined using direct methods.[37] All non-H atoms were refined anisotropically by least-squares techniques.[38] The hydrogen positions were completely retrieved from the differential Fourier card and refined isotropically.[38] The compounds $^3_\infty$[LnCl$_3$(1,4-Ph(CN)$_2$)] with Ln = Sm (**1**)−Tb (**3**) are isotypic and crystallize in the orthorhombic space group *Pnma*, $^3_\infty$[Y$_2$Cl$_6$(1,4-Ph(CN)$_2$)] (**4**) crystallizes in the triclinic space group $P\bar{1}$, and [Y$_2$Cl$_6$(PhCN)$_6$] (**5**) in the monoclinic space group $P2_1/c$. Integrity of symmetry and extinction were checked.[39] Numerical absorption corrections were applied to all five compounds.[40] For **2**, **4**, and **5** the shape of the crystals was determined on the diffractometer and the referring *h,k,l* and orientation were used for the absorption correction. For **1** and **3** the crystal shapes were adjusted to the habitus of the real crystals and refined thereafter.[41] Crystallographic data are summarized in Table 1. Further information was deposited at the Cambridge Crystallographic Data Centre, CCDC, 12 Union Road, Cambridge CB2 1EZ, UK (fax: +44 1223336033 or e-mail: deposit@ccdc.cam.ac.uk) and may be requested by citing the deposition numbers CCDC-677326 (**1**), 677329 (**2**), 677327 (**3**), 677325 (**4**), 677328 (**5**), the names of the authors, and the literature citation.

Of the MOFs **1**−**4** powder patterns were simulated on the basis of the X-ray single crystal data and compared to diffractograms of powder samples of the products. The diffractograms show the products as the main phases. Refinements of the lattice parameters were done on all diffractograms. The cell constants of **1**−**3** were refined on a number of reflections with the best possible resolution leading to an orthorhombic unit cell without unindexed lines. For **1**, 16 reflections with an average $\delta(2\Theta)$ of 0.014° were used (T = 293(2) K, a = 7.173(5) Å, b = 22.204(9) Å, c = 6.375(3) Å, V = 1015.3(7) Å^3); for **2**, 10 reflections were used with an average $\delta(2\Theta)$ of 0.016° (T = 293(2) K, a = 7.124(4) Å, b = 22.166(14) Å, c = 6.338(6) Å, V = 1000.8(8) Å^3)); and for **3**, 16 reflections with an average $\delta(2\Theta)$ of 0.015° were used (T = 293(2) K, a = 7.102(8) Å, b = 22.154(23) Å, c = 6.341(5) Å, V = 997.7(12) Å^3). For **4**, a triclinic cell was refined on 9 reflections with an average $\delta(2\Theta)$ of 0.014° (T = 293(2) K, a = 6.645(8) Å, b = 6.85(4) Å, c = 9.535(3) Å, α = 82.5(4)°, β = 76.03(2)°, γ = 73.48(2)°, V = 403.2(3) Å ^{3}).[42] In addition for the terbium containing MOF **3** a Rietveld refinement was performed with the GSAS package.[43,44] Rietveld refinement also leads to an orthorhombic unit cell (a = 7.0972(5) Å, b = 22.1238(17) Å, c = 6.3417(5) Å and V = 995.75(14) Å^3).

The diffractograms further exhibit secondary phases. For the samarium containing MOF **1** the secondary phase was identified as SmOCl. This proved an impurity of the reagent $SmCl_3$ from the ammonium halide synthesis route.[36] For the gadolinium and terbium

(37) Sheldrick, G. M. *SHELXS-97, Program for the resolution of Crystal Structures*; University of Göttingen: Göttingen, Germany, 1997.
(38) Sheldrick, G. M. *SHELXL-97, Program for the refinement of Crystal Structures*; University of Göttingen: Göttingen, Germany, 1997.
(39) Spek, A. L. *PLATON-2000, A Multipurpose Crystallographic Tool*; Utrecht University: Utrecht, The Netherlands, 2000.
(40) STOE Software Package, V.1.16, X-RED, Program for the numerical absorption correction,Darmstadt, 2001.
(41) *STOE Software Package, V.1.16, X-Shape, Program for the crystal habitus*; STOE: Darmstadt, Germany, 2001.
(42) *STOE WINXPOW v.2.12, Program Package for the Operation of Powder Diffractometers and Analysis of Powder Diffractograms*; STOE: Darmstadt, Germany, 2005.
(43) Larson, A. C.; Dreele, R. B. V.; *General structure analysis system (GSAS)*, Los Alamos National Laboratory Report LAUR 86-748; Los Alamos National Laboratory: Los Alamos, NM, 2000.
(44) Finger, L. W.; Cox, D. E.; Jephcoat, A. P. *J. Appl. Crystallogr.* **1987**, *20*, 79–83.

Table 1. Crystallographic Data for $^{3}_{\infty}[LnCl_3(1,4\text{-}Ph(CN)_2)]$, Ln = Sm (**1**), Gd (**2**), Tb (**3**), $^{3}_{\infty}[Y_2Cl_6(1,4\text{-}Ph(CN)_2)]$ (**4**), $[Y_2Cl_6(PhCN)_6]$ (**5**)[a]

	(1)	(2)	(3)	(4)	(5)
formula	$C_8Cl_3H_4N_2Sm$	$C_8Cl_3H_4N_2Gd$	$C_8Cl_3H_4N_2Tb$	$C_8Cl_6H_4N_2Y_2$	$C_{42}Cl_6H_{30}N_6Y_2$
fw/(g mol^{-1})	384.85	391.74	393.41	518.66	1009.24
crystal system		orthorhombic		triclinic	monoclinic
space group		*Pnma*		$P\bar{1}$	$P2_1/c$
a/Å	7.172(1)	7.116(2)	7.090(2)	6.653(2)	9.767(2)
b/Å	22.209(3)	22.147(4)	22.140(4)	6.799(2)	12.304(3)
c/Å	6.375(1)	6.345(2)	6.325(2)	9.484(2)	19.110(4)
α				81.78(3)°	−
β				76.26(3)°	92.25(3)°
γ				73.29(3)°	−
V/(Å^3)	1015.4(3)	1000.0(3)	992.8(3)	397.9(2)	2294.8(8)
Z		4		1	2
$d_{calc.}$/(g cm^{-1})	2.517	2.602	2.632	2.165	1.461
μ/cm^{-1}	65.3	73.9	78.8	82.4	29.0
T/K			170(2)		
data range	$6.64 \le 2\theta \le 53.98$	$3.68 \le 2\theta \le 54.58$	$3.68 \le 2\theta \le 54.46$	$4.44 \le 2\theta \le 59.05$	$3.94 \le 2\theta \le 54.60$
X-ray radiation			Mo Kα, $\lambda = 71.073$		
no. unique reflections	1070	1134	1126	2187	5084
no. of parameters		75		90	308
R_1 [b] for *n* reflections $F_o > 4\sigma(F_o)$; *n*	0.032; 838	0.033; 844	0.025; 874	0.027; 1919	0.041; 2636
R_1 (all)	0.046	0.040	0.035	0.032	0.089
wR_2 [c] (all)	0.079	0.085	0.061	0.069	0.092
electron density /(e/pm 10^6)	+1.1/−1.9	+0.9/−2.3	+0.9/−2.0	+0.6/−0.9	+0.7/−1.2

[a] Deviations are given in brackets. [b] $R_1 = \sum||F_o| - |F_c||/\sum|F_o|$. [c] $wR_2 = (\sum w(F_o^2 - F_c^2)^2/(\sum w(F_o^4))^{1/2}$.[38]

Chart 1. Reaction of Rare Earth Trichlorides with Dicyanobenzene (1,4-$(Ph(CN)_2$) to Three-Dimensional Framework Structures **1**−**3** with Ln−Cl Layers Interlinked by 1,4-$(Ph(CN)_2$ Ligands

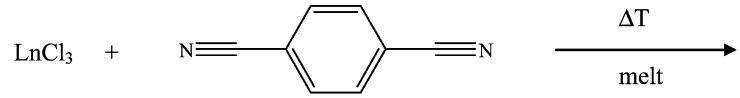

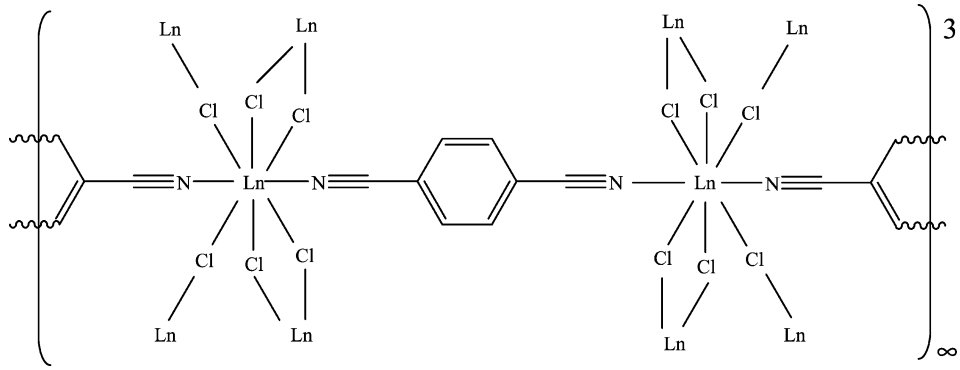

containing MOFs **2** and **3** both indexing of the powder patterns and Rietveld refinement show a weak unknown secondary phase that is neither one of the reagents nor LnOCl. It was also checked for possible isotypic variants of **4** with no result. An analogous observation was made for the powder diffractogram of the bulk sample of the yttrium framework **4**, namely, the weak secondary phase next to **4** is not an isotypic variant of **1**−**3**. Attempts to isolate and crystallize the unknown secondary phase are under way (see Supporting Information for selected powder patterns and the Rietveld plot).

Results and Discussion

A. Formation of First Dinitrile Frameworks of the Rare Earth Elements with the Focus of a High Temperature Reaction Route to MOFs. Despite their different chemical character nearly all MOFs have been synthesized from a solvent treatment.[1−22] This includes the chemistry of the lanthanides. Because of their highly oxophilic character, the use of oxygen containing ligands results in various carboxylates, alcoholates, and nitrates.[12−22,45] To obtain rare earth MOFs that exhibit coordination by nitrogen atoms only, for example, with amide ligands, the absence of oxygen containing ligands and solvents is mandatory. Therefore we developed a solvent free synthesis strategy that involves reaction of the rare earth metals with melts of amines.[27−31] The first rare earth amide MOFs were successfully synthesized by reactions in melts of imidazole, triazole, and triazolopyridine.[23−26]

Nitrile ligands possess strong N donor properties and are therefore suitable to coordinate lanthanide atoms as several

(45) Reinecke, T. M.; Eddaoudi, M.; O′Keeffee, M.; Yaghi, O. M. *Angew. Chem.* **1999**, *111*, 2712–2716.

acetonitrile[46−49] and benzonitrile complexes[50,51] show. However, as nitrile functional groups are redox inactive, a redox reaction is not an option to obtain nitrile complexes. As we show here, melt reactions of nitriles with chlorides of the rare earth elements can be utilized to avoid a redox process and thereby ligand decomposition. Starting with trivalent chlorides and no redox reaction observed all compounds also contain trivalent rare earth ions. Mono nitriles with only one functional group have not been successfully used to build up framework structures. Implementing a second nitrile group by the use of dinitrile ligands enables linkage of lanthanide centers and thus the construction of coordination polymers and framework structures derived from the high temperature syntheses. Chart 1 exemplarily depicts the reactions yielding **1**−**3**.

B. Crystal Structure Investigations on $^3_\infty$[LnCl$_3$(1,4-Ph(CN)$_2$)], Ln = Sm, Gd, Tb, $^3_\infty$[Y$_2$Cl$_6$(1,4-Ph(CN)$_2$)], and [Y$_2$Cl$_6$(PhCN)$_6$]. Single crystal X-ray investigations were applied to all five compounds to evidently show that $^3_\infty$[LnCl$_3$(1,4-Ph(CN)$_2$)] with Ln = Sm (**1**)−Tb (**3**) and $^3_\infty$[Y$_2$Cl$_6$(1,4-Ph(CN)$_2$)] (**4**) have MOF structures, whereas the benzonitrile complex [Y$_2$Cl$_6$(PhCN)$_6$] (**5**) does not exhibit a framework structure. **1**−**3** crystallize isotypic in the orthorhombic crystal system with space group *Pnma*. Framework **4** only has half the 1,4-Ph(CN)$_2$ content of **1**−**3** and therefore a different crystal structure and topology. Lanthanides are generally known for high coordination numbers and a large variety of coordination polyhedra.[52−55] This also enables a large diversity of possible framework structures.

$^3_\infty$[LnCl$_3$(1,4-Ph(CN)$_2$)], with Ln = Sm (**1**)−Tb (**3**), exhibit a C.N. of eight consisting of six halide atoms each as well as two additional nitrile N atoms, resulting in a double N capped trigonal prism of Cl atoms around Ln. **1**−**3** follow the radii contraction of the lanthanides,[55] whereas the group 3 metal yttrium has a significantly smaller trivalent radius.[55] We consider this responsible for the reduced 1,4-Ph(CN)$_2$ content as **4** shows a C.N. of only seven by mono capped trigonal prisms. Furthermore Cl and N atoms in the caps and vertexes of the coordination polyhedron in $^3_\infty$[Y$_2$Cl$_6$(1,4-Ph(CN)$_2$)] (**4**) are switched compared to $^3_\infty$[LnCl$_3$(1,4-Ph(CN)$_2$)] (**1**−**3**). Figure 1 displays the coordination of the Ln atoms in **1**−**3**, and Figure 2 displays the coordination of the Y atoms in **4**. [Y$_2$Cl$_6$(PhCN)$_6$] (**5**) matches with **4** in the

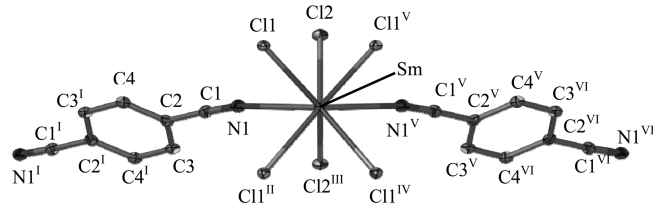

Figure 1. Two-fold nitrile capped trigonal prismatic coordination of chlorine atoms around lanthanide ions in $^3_\infty$[SmCl$_3$(1,4-Ph(CN)$_2$)] (**1**). In these and the following figures the thermal ellipsoids represent 50% of the probability level of the atoms. H atoms are left out for clarity. Symmetry operations: I: $1-x, -y, 2-z$; II: $1/2+x, y, 1/2-z$; III: $1/2+x, 1/2-y, 3/2-z$; IV: $1/2+x, 1/2-y, 1/2-z$; V: $x, 1/2-y, z$; VI: $1-x, 1/2+y, 2-z$.

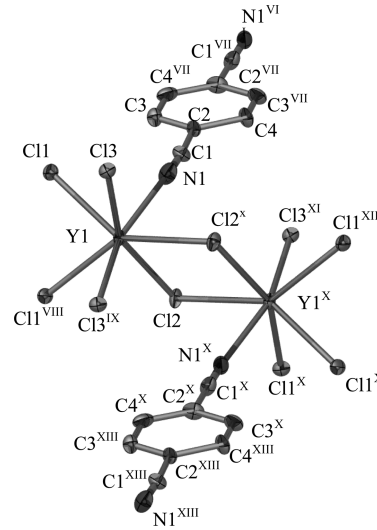

Figure 2. Mono chlorine capped trigonal prismatic coordination of chlorine and nitrile N atoms around yttrium in $^3_\infty$[Y$_2$Cl$_6$(1,4-Ph(CN)$_2$)] (**4**). Symmetry operations: VII: $1-x, 1-y, 2-z$; VIII: $-x, 1-y, 1-z$; IX: $-x, -y, 1-z$; X: $1-x, -y, 1-z$; XI: $1+x, y, z$; XII: $1+x, y-1, z$; XIII: $x, y-1, z-1$.

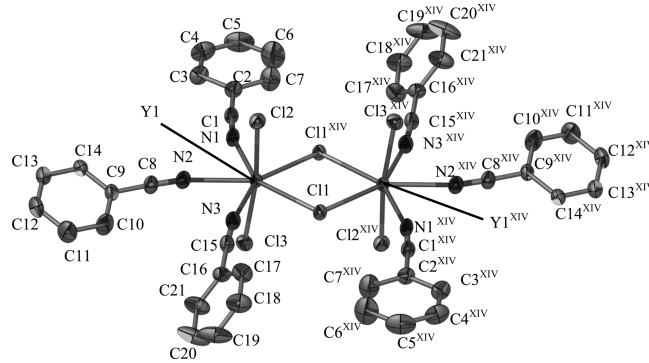

Figure 3. Edge sharing pentagonal bipyramids of chlorine and nitrile N atoms coordinating yttrium in dimeric [Y$_2$Cl$_6$(PhCN)$_6$] (**5**). Symmetry operation: XIV: $2-x, 2-y, -z$.

C.N as it is also seven but exhibits pentagonal bipyramids of four chlorine atoms and three nitrogen atoms of three different benzonitrile ligands. This gives a dimeric complex with one common edge of Cl atoms (see Figure 3). The Ln−Cl distances of **1**−**5** match well with expected values for the trivalent state.[55] The Ln−N distances of **1**−**4** are about 10 pm shorter than in comparable mono nitrile complexes. (Sm−N (**1**): 2.637(6) Å, Sm−Cl: 2.736(2)−2.810(1) Å; Gd−N(**2**): 2.617(5) Å, Gd−Cl: 2.712(2)−2.787(1) Å; Tb−N (**3**): 2.612 (4) Å, Tb−Cl: 2.697(3)−2.777(1) Å;

(46) White, J. P., III.; Deng, H.-B.; Boyd, E. P.; Gallucci, J.; Shore, S. G. *Inorg. Chem.* **1994**, *33*, 1685–1694.
(47) Deacon, G. B.; Görtler, B.; Junk, P. C.; Lork, E.; Mews, R.; Petersen, J.; Zemva, B. *J. Chem. Soc., Dalton Trans.* **1998**, 3887–3891.
(48) White, J. P., III.; Deng, H.-B. J.; Shore, S. G. *J. Am. Chem. Soc.* **1989**, *111*, 8946–8947.
(49) Evans, W. J.; Greci, M. A.; Ziller, J. W. *Inorg. Chem.* **2000**, *39*, 3213–3220.
(50) Quitmann, C. C.; Müller-Buschbaum, K. *Z. Anorg. Allg. Chem.* **2004**, *630*, 573–578.
(51) Balashova, T. V.; Khoroshenkov, G. V.; Kuzyaev, D. M.; Ermenko, I. L.; Aleksandrov, G. G.; Fukin, G. F.; Bochkarev, M. N. *Russ. Chem. Bull.* **2004**, *53*, 825–829.
(52) Dehnicke, K.; Greiner, A. *Angew. Chem.* **2003**, *115*, 1378–1392; *Angew. Chem., Int. Ed.* **2003**, *42*, 1340−1354.
(53) Schumann, H. *Angew. Chem., Int. Ed. Engl.* **1984**, *23*, 474–492; *Angew. Chem.* **1984**, *96*, 475−493.
(54) Schumann, H.; Meese-Marktscheffel, J. A.; Esser, L. *Chem. Rev.* **1995**, *95*, 865–986.
(55) Shannon, R. D. *Acta Crystallogr.* **1976**, *A32*, 751–767.

Table 2. Selected Distances (Å) and Angles (deg) between Atoms of $^3_\infty$[$LnCl_3$(1,4-Ph(CN)$_2$)], Ln = Sm (**1**), Gd (**2**), Tb (**3**), $^3_\infty$[Y_2Cl_6(1,4-Ph(CN)$_2$)] (**4**), and [Y_2Cl_6(PhCN)$_6$] (**5**)[a,b,c,d,e,f]

atoms	(1)	(2)	(3)
Ln−N1	2.637(6)	2.617(5)	2.612(4)
Ln−N1^{V}	2.637(6)	2.617(5)	2.612(4)
Ln−Cl1	2.787(2)	2.769(2)	2.755(1)
Ln−Cl1^{V}	2.810(2)	2.787(2)	2.777(1)
Ln−Cl2	2.757(3)	2.728(2)	2.714(2)
Ln−Cl2^{III}	2.736(2)	2.712(2)	2.697(2)
N1−Ln−N1^{V}	129.3(2)	129.7(2)	129.8(2)
N1−Ln−Cl2	70.6(2)	70.6(2)	70.7(1)
C1−N1−Ln	166.8(5)	166.8(5)	166.9(4)
N1−C1−C2	177.2(8)	177.2(6)	177.4(5)

atoms	(4)	atoms	(5)
Y−N1	2.466(3)	Y−N1	2.450(4)
Y−Cl1	2.683(2)	Y−N2	2.485(4)
Y−Cl1^{VIII}	2.692(2)	Y−N3	2.484(4)
Y−Cl2	2.650(1)	Y−Cl1	2.704(2)
Y−Cl2^{X}	2.747(2)	Y−Cl2	2.571(2)
Y−Cl3	2.693(1)	Y−Cl3	2.581(2)
Y−Cl3^{IX}	2.698(2)	Y−Cl1X^{XIII}	2.721(2)
N1−C1	113.9(5)	N1−Y−N2	73.6(2)
N1−Y−Cl1	122.8(8)	Cl2−Y−Cl3	170.7(4)
N1−Y−Cl3	90.6(8)	Cl2−Y−Cl1	91.2(4)
Y−N1−C1	154.9(3)	C1−N1−Y	163.4(3)
N1−C1−C2	176.6(4)	N1−C1−C2	174.6(5)

[a] Deviations are given in brackets. [b] V: Symmetry operation: x, 1/2 − y, z. [c] III: Symmetry operation: 1/2 + x, 1/2 − y, 3/2 − z. [d] X: Symmetry operation: 1 − x, −y, 1 − z. [e] IX: Symmetry operation: −x, −y, 1 − z. [f] XIII: Symmetry operation: x, y − 1, z − 1.

Y−N(**4**): 2.466(3)) Å, Y−Cl: 2.650(1)−2.747(2) Å; Y−N(**5**): 2.467(4) Å, Y−Cl: 2.650(1)−2.698(2) Å). This can be explained by a weakening of the donor bond by each ligand coordinating with both nitrile groups in the MOFs **1**−**4** and not just one nitrile group as in **5**. In comparison [$Sm(MeCN)_9$][AsF_6]$_3$ exhibits Sm−N nitrile distances of 2.52−2.55 Å,[47] [$Gd((NH_2)_2CO)_4(H_2O)_2Cr(CN)_6$]$_2$ exhibits Gd−N cyanide distances of 2.50−2.51 Å,[56] [$Tb(NCNC(NH_2)_2)_2(H_2O)_6$]$Cl_3$ shows a Tb−N distance of 2.45 Å,[57] and finally [$Y((Me_3Si)_2N)_3(PhCN)_2$] exhibits Y−N nitrile distances of 2.47−2.49 Å.[58] Illuminated by the interatomic distances and angles the Tb network **3** already exhibits a strong distortion of the coordination polyhedra. For the smaller Y^{III} cation in **4** a reduction of the C.N. takes place. See Table 2 for a selection of interatomic distances and angles of **1**−**5**.

As [Y_2Cl_6(PhCN)$_6$] (**5**), [$DyI_3(PhCN)_4$]·0.5PhCN,[51] as well as [Ho_2Cl_6(PhCN)$_6$], $^2_\infty$[$HoCl_3$(PhCN)],[50] and [$Y((Me_3Si)_2N)_3(PhCN)_2$,[58] illustrate, the mono nitrile ligand coordinates end-on to only one metal center. There is no option for an inter linkage between two rare earth centers via a single nitrile ligand. Because only the Cl atoms allow linkages through μ_2 bridging, no three-dimensional (3D) frameworks are accessible. The highest known dimensionality for homo metallic mono nitriles of the rare earth elements has been observed for $^2_\infty$[$HoCl_3$(PhCN)], which consists of 2D-{$HoCl_{6/3}$} nets.[50] In contrast the 1,4-Ph(CN)$_2$ ligand allows front and backside coordination with an Ln−1,4-Ph(CN)$_2$−Ln angle of 180 °. The benzodinitrile ligand henceforth contributes to the dimensionality of the network and is responsible for the construction of 3D frameworks in **1**−**4**. Two of the dimensions constitute the Ln−Cl layers, the third direction is built up by the 1,4-Ph(CN)$_2$ ligands, which also function as spacers between the Ln−Cl planes. The spacer distance is a vital point in MOF structures. For $^3_\infty$[$LnCl_3$(1,4-Ph(CN)$_2$)], with Ln = Sm (**1**)−Tb (**3**), the distances between the planes are 7.80 Å for **1**, 8.10 Å for **2**, and 8.15 Å for **3**. As this is less than the extension of a double metal bonded 1,4-Ph(CN)$_2$ ligand, the interatomic angles N−Ln−N between the ligands ranges from 129.5(2) ° for Sm in (**1**) to 130.0(4) ° for Tb in (**3**) instead of 180 °. This causes an intercrossing of 1,4-Ph(CN)$_2$ ligands and a better packing instead of a vertical arrangement of the ligands regarding the *b* axis. This results in cavities with diameters of 3.96−6.82 Å for **1**, 3.90−6.18 Å for **2**, and 3.43−6.72 Å for **3**. Figure 4 displays the crystal structure of $^3_\infty$[$LnCl_3$(1,4-Ph(CN)$_2$)], Ln = Sm (**1**)−Tb (**3**).

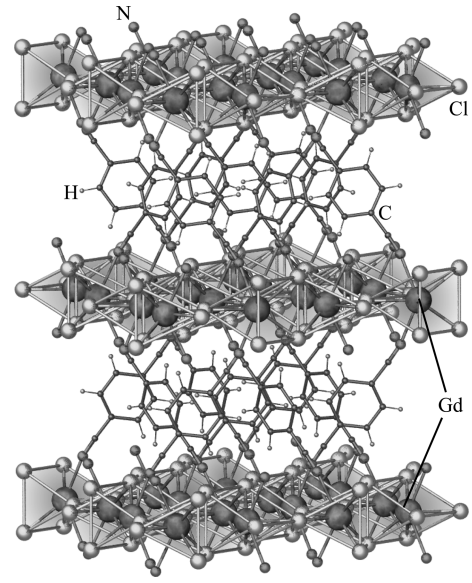

Figure 4. Crystal structure of the MOF $^3_\infty$[$GdCl_3$(1,4-Ph(CN)$_2$)] (**2**). The structure consists of Gd−Cl layers that are connected by the nitrile groups of 1,4-(Ph(CN)$_2$ molecules. Lines between the nitrogen atoms do not represent bonds but the coordination polyhedra.

$^3_\infty$[Y_2Cl_6(1,4-Ph(CN)$_2$)] (**4**) has a related structure of Y−Cl layers as well as showing the linkage of the layers via 1,4-Ph(CN)$_2$ ligands constituting the framework structure. The arrangement of Cl and N atoms in caps and vertexes of the capped trigonal prisms causes a different constitution of the Y−Cl layers compared to **1**−**3**. The lower C.N. together with the reduced amount of 1,4-Ph(CN)$_2$ ligands moreover thins the linkages in the third dimension by one half so that no alternating orientations of the 1,4-Ph(CN)$_2$ molecules result. All linkers head into the same direction. The resulting distance of the Y−Cl layers after subtractions of the covalent radii is 7.67 Å and cavities in the structure with diameters between 4.95 and 8.05 Å referring to van-der-Waals radii. Figure 5 depicts the crystal structure of $^3_\infty$[Y_2Cl_6(1,4-Ph(CN)$_2$)] (**4**).

(56) Khou, H.-Z.; Gao, S.; Li, C.-H.; Liao, D.-Z.; Zhou, B.-C.; Wang, R.-J.; Li, Y. *Inorg. Chem.* **2002**, *41*, 4756–4762.
(57) Liao, W.; Hu, C.; Dronskowski, R. *Acta Crystallogr.* **2003**, *E59*, m1124–m1126.
(58) Westerhausen, M.; Hartmann, M.; Pfitzner, A.; Schwarz, W. *Z. Anorg. Allg. Chem.* **1995**, *921*, 837–850.

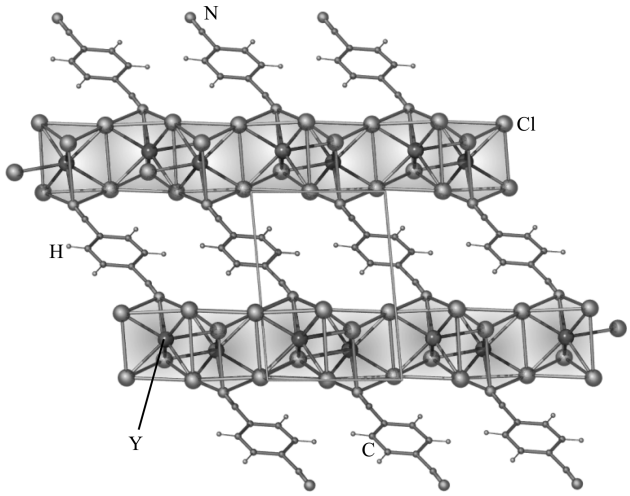

Figure 5. Crystal structure of the MOF $^3_\infty$[Y_2Cl_6(1,4-Ph(CN)$_2$)] (**4**). The structure consists of canted Y−Cl layers that are connected by the nitrile groups of 1,4-(Ph(CN)$_2$ molecules. Density of 1,4-(Ph(CN)$_2$ in **4** is only one half that of **1**−**3**.

Because of their different ligand content, $^3_\infty$[$LnCl_3$(1,4-Ph(CN)$_2$)], with Ln = Sm (**1**)−Tb (**3**), and $^3_\infty$[Y_2Cl_6(1,4-Ph(CN)$_2$)] (**4**) also have different topologies. $^3_\infty$[$LnCl_3$(1,4-Ph(CN)$_2$)] **1**−**3** can be described as a 4,6 net[59] comparable to the topology of the structure of VF_3. As Chart 2 shows, the MOFs **1**−**3** can also be described by two two-dimensional (2D)-nets: one nearly ideal horizontal 2D (4,4) net of the Ln−Cl layers, and a canted perpendicular (6,4) net for the additional nitrile connections. This is a simplified network topology. To fully include the high connectivity of the lanthanide ions in **1**−**3** (8:8 coordination:connectivity) the alternation of edge and corner μ_2 connected trigonal Cl prisms requires the insertion of "double bridges"[15] for half of the chlorine connections. The resulting overall lattice symbol would be 4,8 of two perpendicular 2D nets that have a 2-fold higher connectivity of (4,6) and (6,6) (see Chart 2).[15]

Considering a simplified topology and no double bridges in the first instance, $^3_\infty$[Y_2Cl_6(1,4-Ph(CN)$_2$)] (**4**) consists of two 2D-nets: a 2D (6,3) net of the Y−Cl layers with a graphite analogous conformation and perpendicular layers including the dinitrile ligands that also constitute to a 2D (6,3) net. Thus an overall net symbol of 6,4[59] results for the 3D network. Chart 3 depicts a schematic representation of the topology of **4**. For an interpretation including the full Y connectivity and hence "double bridges"[15] for μ_2 chlorine connections the network can be described as a 2D (6,6) net for the Y−Cl layers and a perpendicular 2D (6,5) net for the layers including the dinitrile ligands. Thus an overall lattice symbol of 6,7 results for a complete description of the topology of the 3D framework **4** (see Chart 3).[15]

A comparison with the literature shows that these topologies are not found for halide or N-coordinated framework structures. Though the 2D topologies (4,4) and (6,3) were long described by Wells[59] there are only two examples for the 3D topology 4,8 of **1**−**3**, both being zinc carboxylates:[60,61] {[Zn(nicotinate)$_2$]·MeOH·2H_2O}*n* and [Zn(BTEC)$_{1/2}$]*n* (BTEC = 1,2,4,5-benzenetetracarboxylate). To the best of our knowledge no example is found for the 6,7 topology of compound **4**.

Chart 2. Depiction of the Connectivity and Topology of the Framework $^3_\infty$[$LnCl_3$(1,4-Ph(CN)$_2$)], Ln = Sm (**1**)−Tb (**3**)[a]

[a] Dark lines represent "double-bridges" within the full connectivity description of the topology.

C. Spectroscopic and Thermal Investigations and Considerations. The dinitrile MOFs $^3_\infty$[$LnCl_3$(1,4-Ph(CN)$_2$)], with Ln = Sm (**1**)−Tb (**3**), $^3_\infty$[Y_2Cl_6(1,4-Ph(CN)$_2$)] (**4**), and the mononitrile [Y_2Cl_6(PhCN)$_6$] (**5**) were investigated spectroscopically with MIR, FIR and Raman techniques. Both FIR and Raman spectra show a series of bands that cannot be identified with the neutral ligands[62,50] and represent the Ln−N stretching modes (FIR: Sm (**1**): 275, 234, 207; Gd (**2**): 273, 229, 206; Tb (**3**): 279, 232, 207; Y (**4**): 275, 224, 191; Y (**5**): 218, 150 cm^{-1}). For the group 3 metal Y (**4**,**5**) the FIR bands are shifted in comparison to the respective bands of the lanthanides. All are in the region of known

(59) Wells, A. F. *Three-dimensional nets and polyhedra*; Wiley-Interscience: New York, 1977.
(60) Rather, B.; Moulton, B.; Bailey Walsh, R. D.; Zaworotko, M. J. *Chem. Commun.* **2002**, *7*, 694–695.
(61) Wen, Y.-H.; Wen, J.-H.; Zhang, Q.-W.; He, J.-H.; Feng, Y.-L. *Inorg. Chem. Commun.* **2007**, *10*, 10543–10546.
(62) Schrader, B. *Raman/Infrared Atlas of Organic Compounds*, 2nd ed.; Wiley VCH: 1989.
(63) Haghighi, M. S.; Teske, C. L.; Homborg, H. *Z. Anorg. Allg. Chem.* **1992**, *608*, 73–80.
(64) Freeman, H. C.; Snow, M. R. *Acta Crystallogr.* **1965**, *18*, 843–845.
(65) Müller-Buschbaum, K.; Quitmann, C. C. *Inorg. Chem.* **2003**, *42*, 2742–2750.

Chart 3. Depiction of the Connectivity and Topology of the Framework $^3_\infty[Y_2Cl_6(1,4\text{-}Ph(CN)_2)]$ (**4**)[a]

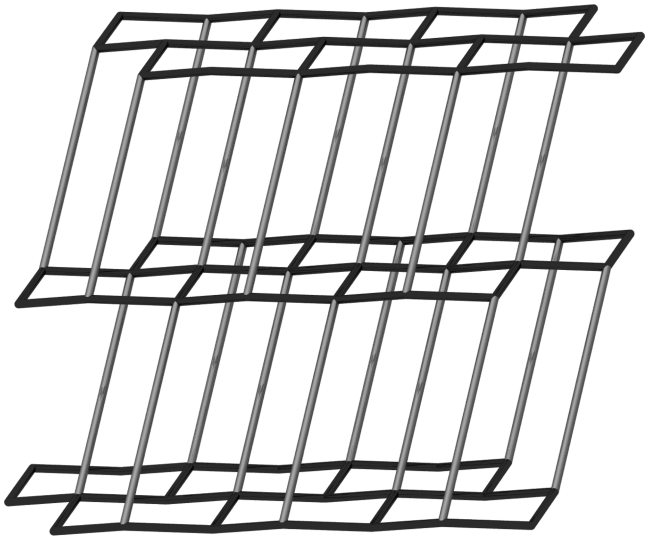

[a] Dark lines represent "double-bridges" within the full connectivity description of the topology.

Ln−N vibrations.[27,24−26,28−31,63−68] Because most investigations on Ln nitrile complexes lack referring FIR spectra,[47,58,69−72] the benzonitrile complexes $[Ho_2Cl_6(PhCN)_6]$ and $^2_\infty[HoCl_3(PhCN)]$[50] mark sparse examples for a direct comparison. They exhibit Ho−N vibrations in the region 270−180 cm^{-1}. The strong vibration bands between 570−480 cm^{-1} (FIR and MIR: Sm (**1**): 542; Gd (**2**): 565, 542; Tb (**3**): 563, 530; Y (**4**): 566, 550, 540; Y (**5**): 552, 492 cm^{-1}) can be identified with the asymmetric Ln−Cl vibrations,[68,72] the strong bands between 2230−2300 cm^{-1} with υ(C−N) of the nitrile groups (MIR: Sm (**1**): 2260, 2233; Gd (**2**): 2263, 2233; Tb (**3**): 2258, 2233; Y (**4**): 2261; Y (**5**): 2267).

Simultaneous DTA and TG[73] (NETZSCH STA-409) measurements were carried out to investigate the thermal behavior of $^3_\infty[LnCl_3(1,4\text{-}Ph(CN)_2)]$ on the samarium containing MOF **1** as an exemplary. Therefore, the product was purified by evaporating excess 1,4-$(Ph(CN)_2$ at 200 °C. A 32.7 mg quantity of **1** was heated from 20 to 700 °C in a constant Ar flow of 60 mL/min with a heating rate of 15 °C/min. The investigation shows that the purified products contain not more but neglectible amounts of excess 1,4-$(Ph(CN)_2$) as no melting point of the ligand is observed. Instead a small amount (2%) of PhCN is released at 185 °C (signal (1); exp. bp.: 191−193 °C). **1** shows a two step

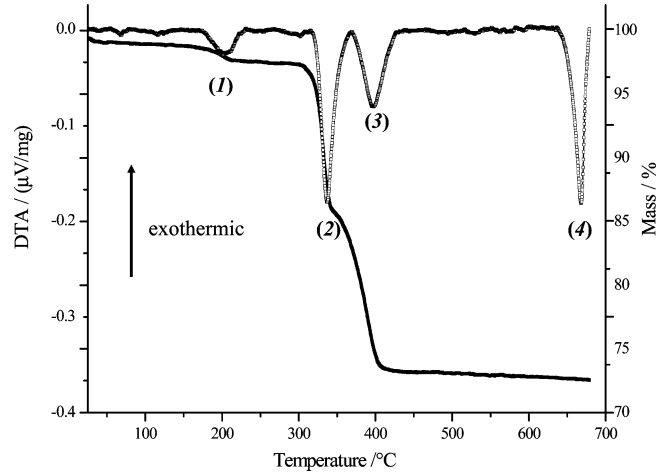

Figure 6. Thermal analysis of $^3_\infty[SmCl_3(1,4\text{-}Ph(CN)_2)]$ (**1**) investigated by simultaneous DTA/TG in the temperature range of 20 to 700 °C with a heating rate of 15 °C/min in a continuous Ar flow of 60 mL/min. Signal (1), bp benzonitrile; signals (2) and (3), decomposition of the network; signal (4), mp $SmCl_3$.

decomposition under release of 1,4-$(Ph(CN)_2$ in both steps (signal (2): 321; signal (3): 375 °C, 24%). The detected mass loss corresponds to the expected value for the 1,4-$(Ph(CN)_2$ ligand of 24%. It results in formation of $SmCl_3$ (mp. signal (4): 670 °C; exp.: 686 °C). See Figure 6 for the course of the thermal decomposition of **1**. Ln dinitrile MOFs have a competitive intrinsic thermal stability compared to carboxylates as they are not prone to the release of CO_2. Hence, they could be interesting for applications that imply an extended thermal stability, and they withstand sorption energies better than carboxylates, as well as enabling purification by evaporation of excess organic components.

Conclusions

Synthesis strategies from solid state chemistry, particularly solvent free reactions with a melt of an organic ligand, can successfully be used to obtain MOF structures. It is an exceptionally useful concept to prepare rare earth framework structures with non-oxygen containing ligands and has now been transferred from Ln amide MOFs to Ln nitrile MOFs by the results on the 1,4-$(Ph(CN)_2$ constituted frameworks $^3_\infty[LnCl_3(1,4\text{-}Ph(CN)_2)]$, Ln = Sm (**1**)−Tb (**3**) and $^3_\infty[Y_2Cl_6(1,4\text{-}Ph(CN)_2)]$ (**4**). The 1,4-$(Ph(CN)_2$ ligand is responsible for connection of the Ln−Cl layers to 3D-networks. Because of the extension of the ligand and despite of a non-180 ° linear end-on metal coordination, the structures contain cavities with diameters ranging between 3.9 and 8.0 Å. Without the second functional group no MOF formation is observed as $[Y_2Cl_6(PhCN)_6]$ (**5**) and other mononitriles with acetonitrile and benzonitrile confirm. Within the dinitrile MOFs **1**−**4** the lanthanide and group 3 metals adopt large coordination numbers that result in topologies of the networks with high connectivity and complexity. The variety of rare earth elements and ionic radii between the smallest Sc^{3+} and the largest La^{3+} lets us assume that more MOF structures with interesting structures and topologies are available, especially if other halides and dinitriles are considered too. The 1,3-$(Ph(CN)_2$ (*iso*-phthalic acid dinitrile) offers even

(66) Müller-Buschbaum, K.; Mokaddem, Y. *Inorg. Chem.* **2003**, *42*, 2742–2750.
(67) Müller-Buschbaum, K. *Z. Anorg. Allg. Chem.* **2002**, *628*, 2731–2737.
(68) Weidlein, J.; Müller, U.; Dehnicke, K. *Schwingungsfrequenzen II, Nebengruppenelemente*; Georg Thieme Verlag, 1986.
(69) Errington, W.; Spry, M. P.; Willey, G. R. *Acta Crystallogr.* **1998**, *C54*, 290–291.
(70) Chebulo, V.; Whitle, R. R.; Sen, A. *Inorg. Chem.* **1985**, *24*, 3082–3087.
(71) Willey, G. R.; Aris, D. R.; Errington, W. *Inorg. Chim. Acta* **2001**, *318*, 97–102.
(72) *Handbook of the Physics and Chemistry of Rare Earths*; Haschke, J. M., Gschneider, K. A., Eyring Le, R., Eds.; Elsevier: North-Holland, 1979; Vol. *4*.
(73) Hemminger, W. F.; Cammenga, H. K. *Methoden der Thermischen Analyse*; Springer Verlag: Berlin, 1989.

more complexity as the two nitrile groups are no longer in 180 ° *para* positions but 120 ° *meta* to each other.

Acknowledgment. We are grateful to the *Deutsche Forschungsgemeinschaft* for funding this work through the project "3D-Raumnetze komplexer Selten-Erd-Amide, ein Weg zu neuartigen MOFs", the *Wilhelm-Klemm* foundation, and the *Evonik-Dr.-Otto-Röhm-Gedächtnis* foundation. We further thank Prof. Dr. D. Johrendt and M. Tegel for their help with the Rietveld refinement.

Supporting Information Available: Tables of atomic coordinates, thermal parameters, atom distances, interatomic angles, and detailed crystallographic data for (**1**−**5**) and additional depictions. This material is available free of charge via the Internet at http://pubs.acs.org.

IC800635U